

# Structure of $A = 7$ iso-triplet $\Lambda$ hypernuclei studied with the four-body cluster model

E. Hiyama

*Nishina Center for Accelerator-Based Science, Institute for Physical and Chemical Research (RIKEN), Wako, Saitama 351-0198, Japan*

Y. Yamamoto

*Physics Section, Tsuru University, Tsuru, Yamanashi 402-8555, Japan*

T. Motoba

*Laboratory of Physics, Osaka Electro-Comm. University, Neyagawa 572-8530, Japan*

M. Kamimura

*Department of Physics, Kyushu University, Fukuoka 812-8581, Japan*

(Received 3 August 2009; published 30 November 2009)

The structure of the  $T = 1$  isotriplet hypernuclei,  ${}^7_\Lambda\text{He}$ ,  ${}^7_\Lambda\text{Li}$ , and  ${}^7_\Lambda\text{Be}$  within the framework of an  $\alpha + \Lambda + N + N$  four-body cluster model is studied. Interactions between the constituent subunits are determined so as to reproduce reasonably well the observed low-energy properties of the  $\alpha N$ ,  $\alpha\Lambda$ ,  $\alpha NN$ , and  $\alpha\Lambda N$  subsystems. Furthermore, the two-body  $\Lambda N$  interaction is adjusted so as to reproduce the  $0^+ - 1^+$  splitting of  ${}^4_\Lambda\text{H}$ . Also, a phenomenological  $\Lambda N$  charge symmetry breaking (CSB) interaction is introduced. The  $\Lambda$  binding energy of the ground state in  ${}^7_\Lambda\text{He}$  is predicted to be 5.16 (5.36) MeV with (without) the CSB interaction. The calculated energy splittings of the  $3/2^+ - 5/2^+$  states in  ${}^7_\Lambda\text{He}$  and  ${}^7_\Lambda\text{Li}$  are around 0.1 MeV. We point out that there is a three-layer structure of the matter distribution,  $\alpha$  particle,  $\Lambda$  skin, and proton or neutron halo, in the  ${}^7_\Lambda\text{He}(J = 5/2^+)$ ,  ${}^7_\Lambda\text{Li}(J = 5/2^+)$ , and  ${}^7_\Lambda\text{Be}(J = 1/2^+)$  states.

DOI: [10.1103/PhysRevC.80.054321](https://doi.org/10.1103/PhysRevC.80.054321)

PACS number(s): 21.80.+a, 21.10.Dr, 21.60.Gx, 21.45.-v

## I. INTRODUCTION

A new stage in hypernuclear physics is opened by the  $\gamma$ -ray spectroscopy for  $\Lambda$  hypernuclei, where level structures of the order of keV are revealed systematically. In order to extract valuable information on hypernuclear structure and the underlying  $\Lambda N$  interactions from these extremely precise data it is, therefore, indispensable to utilize accurate models for the many-body wave functions.

Of special concern in this work is the structure of a multiplet of  $\Lambda$  hypernuclei specified by an isospin  $T$ , which provided us with many interesting subjects so far. For example, in the case of the  $T = 1$  multiplet with mass number  $A = 7$ ,  ${}^7_\Lambda\text{He}$ ,  ${}^7_\Lambda\text{Li}$ , and  ${}^7_\Lambda\text{Be}$ , their core nuclei are neutron or proton halo nuclei. When a  $\Lambda$  particle is added to the core nuclei,  ${}^6\text{He}$ ,  ${}^6\text{Li}$  ( $T = 1$ ), and  ${}^6\text{Be}$ , the resultant hypernuclear systems become more stable against neutron or proton emissions. Hereafter,  $T = 1$  excited states of  ${}^6\text{Li}$  and  ${}^7_\Lambda\text{Li}$  are denoted as  ${}^6\text{Li}^*$  and  ${}^7_\Lambda\text{Li}^*$ . This stabilization is caused by the so-called glue-like role of  $\Lambda$  [1]. As a result of the role of the  $\Lambda$  particle, we can expect the interesting possibility that neutron (proton) drip lines in  $\Lambda$  hypernuclei are extended far away from those in ordinary nuclear systems.

In the past, the level structures in  ${}^7_\Lambda\text{He}$ ,  ${}^7_\Lambda\text{Li}$  ( $T = 1$ ), and  ${}^7_\Lambda\text{Be}$  were studied with the three-body  ${}^5_\Lambda\text{He} + N + N$  model [2], where only the even-state  $\Lambda N$  interaction was used. In Ref. [2], we pointed out that there appear halo or skin structures in the ground state or some excited states of these hypernuclei. Recently, the experimental energy of the  $T = 1$   $J = 1/2^+$  state of  ${}^7_\Lambda\text{Li}$  was observed through the high-resolution  $\gamma$ -ray experiment [3]. Furthermore, it was proposed to produce  ${}^7_\Lambda\text{He}$

by the  $(e, e' K^+)$  reaction at JLAB. One aim of the present work is to discuss halo or skin structures in the extended framework of an  $\alpha + \Lambda + N + N$  four-body model.

Another interesting subject to discuss is the spin-doublet state,  $5/2^+ - 3/2^+$  in  ${}^7_\Lambda\text{He}$  and  ${}^7_\Lambda\text{Li}$  ( $T = 1$ ). It is considered that these excited  $5/2^+ - 3/2^+$  doublets are related intimately to the spin-dependent potentials of the  $\Lambda N$  interaction. Therefore, it is important to discuss these splitting energies to determine the spin-dependent parts of the  $\Lambda N$  interaction.

In our previous work [4], the spin-doublet structures of  ${}^7_\Lambda\text{Li}$  in  $T = 0$  states and the underlying spin-dependent interactions were investigated successfully in the  $\alpha pn\Lambda$  four-body cluster model. Here, the  $\alpha p$  and  $\alpha n$  interactions were chosen so as to reproduce the corresponding phase shifts, and the  $\Lambda\alpha$  interaction was done so as to reproduce the experimental value of  $B_\Lambda({}^5_\Lambda\text{He})$ , and the  $\Lambda N$  spin-spin (spin-orbit) interaction was fitted so as to be consistent with the  $0^+ - 1^+$  ( $5/2^+ - 3/2^+$ ), spin-doublet energy separation in  ${}^4_\Lambda\text{H}$  ( ${}^9_\Lambda\text{Be}$ ). In the present work, our four-body analyses for  ${}^7_\Lambda\text{Li}$  ( $T = 0$ ) are extended straightforwardly to the  $T = 1$  multiplet ( ${}^7_\Lambda\text{He}$ ,  ${}^7_\Lambda\text{Li}^*$ ,  ${}^7_\Lambda\text{Be}$ ), where an asterisk stands for the  $T = 1$  excited states.

An important subject related to the isospin multiplet of  $\Lambda$  hypernuclei is the charge symmetry breaking (CSB) components in  $\Lambda N$  interactions. The most reliable evidence for the CSB interaction appears in the  $\Lambda$  binding energies  $B_\Lambda$  of the  $A = 4$  members with  $T = 1/2$  ( ${}^4_\Lambda\text{He}$  and  ${}^4_\Lambda\text{H}$ ). Then, the CSB effects are attributed to the differences  $\Delta_{\text{CSB}} = B_\Lambda({}^4_\Lambda\text{He}) - B_\Lambda({}^4_\Lambda\text{H})$ , the experimental values of which are  $0.35 \pm 0.06$  MeV and  $0.24 \pm 0.06$  MeV for the ground ( $0^+$ ) and excited ( $1^+$ ) states, respectively. There exist mirror

hypernuclei in the  $p$ -shell region such as the  $T = 1$  multiplet with  $A = 7$  ( ${}^7_{\Lambda}\text{He}$ ,  ${}^7_{\Lambda}\text{Li}^*$ ,  ${}^7_{\Lambda}\text{Be}$ ),  $T = 1/2$  multiplet with  $A = 8$  ( ${}^8_{\Lambda}\text{Li}$ ,  ${}^8_{\Lambda}\text{Be}$ ),  $T = 1/2$  multiplet with  $A = 10$  ( ${}^{10}_{\Lambda}\text{Be}$ ,  ${}^{10}_{\Lambda}\text{B}$ ), and so on. Historically, some authors mentioned CSB effects in these  $p$ -shell  $\Lambda$  hypernuclei [5,6]. However, there is no microscopic calculation of these hypernuclei taking account of the CSB interaction.

It is well known that the experimental values of  $\Delta_{\text{CSB}}$  can be fitted phenomenologically by an effective spin-independent CSB interaction. Nevertheless, in the case of a meson-theoretical model an One Pion Exchange (OPE)-type CSB potential is derived through a  $\Lambda - \Sigma^0$  mixing effect, where the triplet CSB interaction is much stronger than the singlet interaction due to the tensor-force contribution. This feature is in strong disagreement with that in the phenomenological force, which is almost spin-independent. This difference between triplet and singlet CSB interactions appears in the elaborate four-body calculations for  ${}^4_{\Lambda}\text{He}$  and  ${}^4_{\Lambda}\text{H}$  with the use of the Nijmegen soft core model (NSC97e model) [7], in which the CSB components are generated by the mass difference within the  $\Sigma$ -multiplet mixed in  $\Lambda$  states and the  $\Lambda - \Sigma^0$  mixing effect.

Since the origin of the CSB interaction is not yet settled, we treat it phenomenologically in the present study. Similarly to Ref. [8], the CSB interaction is determined so as to reproduce the values of  $\Delta_{\text{CSB}}$  obtained from the  $\Lambda$  binding energies of  ${}^4_{\Lambda}\text{H}$  and  ${}^4_{\Lambda}\text{He}$ . Then, the  $T = 1$  triplet hypernuclei with  $A = 7$  ( ${}^7_{\Lambda}\text{He}$ ,  ${}^7_{\Lambda}\text{Li}^*$ ,  ${}^7_{\Lambda}\text{Be}$ ) are studied with the use of this CSB interaction in the four-body cluster model. Additionally, the CSB effects in the  $T = 1/2$  doublet hypernuclei with  $A = 8$  are investigated within the  $\alpha t \Lambda$  and  $\alpha^3\text{He} \Lambda$  cluster models for  ${}^8_{\Lambda}\text{Be}$  and  ${}^8_{\Lambda}\text{Li}$ , respectively.

In this work, we study  $A = 7$  hypernuclei within the framework of an  $\alpha + \Lambda + N + N$  four-body model so as to take account of the full correlations among all the constituent baryons. Two-body interactions among constituent particles are chosen so as to reproduce all the existing binding energies of the subsystems ( $\alpha N$ ,  $\alpha \Lambda N$ ,  $\alpha \Lambda$ , and so on). This feature is important in the analysis of the energy levels of these hypernuclei. Our analysis is performed systematically for both ground and excited states of  $\alpha \Lambda NN$  systems with no more adjustable parameters in this stage so that these predictions can offer important guidance for the interpretation of upcoming hypernucleus experiments, such as the  ${}^7\text{Li}(e, e' K^+) {}^7_{\Lambda}\text{He}$  reaction at JLAB.

In Sec. II, the microscopic  $\alpha \Lambda NN$  and  $NNN \Lambda$  four-body calculation method is described. In Sec. III the interactions are explained. The calculated results and the discussion are presented in Sec. IV. Section V is devoted to the discussion on the CSB effects obtained for the  $A = 7$  and 8 systems. The summary is given in Sec. VI.

## II. FOUR-BODY CLUSTER MODEL AND METHOD

The models employed in this article are the same as those in our previous work [4]. Namely, we employ the  $\alpha + \Lambda + N + N$  model for the  $A = 7$  hypernuclei (Fig. 1) and the  $\alpha + N + N$  model for the  $A = 6$  nuclei (Fig. 3 in Ref. [4]), where

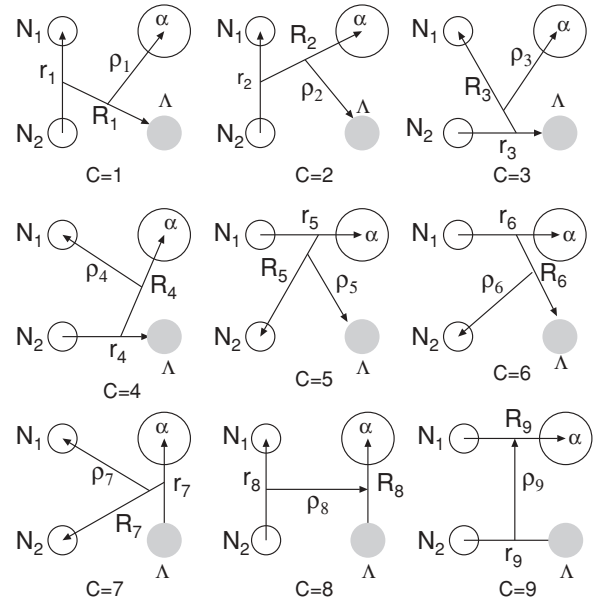


FIG. 1. Jacobi coordinates for all the rearrangement channels ( $c = 1 \sim 9$ ) of the  $\alpha + \Lambda + N_1 + N_2$  four-body system. Two nucleons are to be antisymmetrized.

all the rearrangement channels are taken into account. The Schrödinger equation is given by

$$(H - E) \Psi_{JM, TT_z}({}^7_{\Lambda}\mathbf{Z}) = 0, \quad (2.1)$$

$$H = T + V_{N_1 N_2} + \sum_{i=1}^2 (V_{\Lambda N_i} + V_{\alpha N_i}) + V_{\alpha \Lambda} + V_{\text{Pauli}}, \quad (2.2)$$

where  $V_{\alpha N_i}$  is the interaction between the  $\alpha$  particle and  $i$ th nucleon and  $V_{\alpha \Lambda}$  is the  $\alpha \Lambda$  interaction, which are explained in the next section. The Pauli principle between the  $\alpha$  particle and the two nucleons is taken into account by the Pauli projection operator  $V_{\text{Pauli}}$ , which is the same as in Ref. [4]. The total wave function is described as a sum of amplitudes of all the rearrangement channels shown in Fig. 1 in the LS-coupling scheme:

$$\begin{aligned} \Psi_{JM, TT_z}({}^7_{\Lambda}\mathbf{Z}) = & \sum_{c=1}^9 \sum_{nl, NL, v\lambda} \sum_{IK} \sum_{sS} C_{nl, NL, v\lambda, IK, sS}^{(c)} \Phi(\alpha) \\ & \times \mathcal{A} \{ [ [\phi_{nl}^{(c)}(\mathbf{r}_c) \psi_{NL}^{(c)}(\mathbf{R}_c)]_I \xi_{v\lambda}^{(c)}(\boldsymbol{\rho}_c) ]_K \\ & \times [ [\chi_{\frac{1}{2}}(N_1) \chi_{\frac{1}{2}}(N_2)]_s \chi_{\frac{1}{2}}(\Lambda)]_s ]_{JM} \\ & \times [ \eta_{\frac{1}{2}}(N_1) \eta_{\frac{1}{2}}(N_2) ]_{TT_z} \}, \end{aligned} \quad (2.3)$$

where the notations are the same as in Ref. [4]. Also, the definitions of the Gaussian basis functions and the Gaussian ranges are the same as those in the case of the  $A = 4$  hypernuclei.

The eigenenergy  $E$  in Eq. (2.2) and the  $C$  coefficients in Eq. (2.3) are determined by the Rayleigh-Ritz variational method. The angular momentum space of  $l, L, \lambda \leq 2$  is found to be sufficient to obtain good convergence of the calculated results as described in the following.

### III. INTERACTIONS

#### A. Charge symmetry parts

We recapitulate here the charge symmetric parts of the  $V_{N\alpha}$ ,  $V_{NN}$ ,  $V_{\alpha\Lambda}$ , and  $V_{\Lambda N}$  interactions employed in our  $\alpha NN\Lambda$  systems [4].

For  $V_{N\alpha}$ , we employ the effective potential proposed in Ref. [9], which is designed so as to reproduce well the low-lying states and low-energy scattering phase shifts of the  $\alpha n$  system. The Pauli principle between nucleons belonging to the  $\alpha$  and the valence nucleon is taken into account by the orthogonality condition model (OCM) [10]. As for the  $NN$  interaction  $V_{NN}$ , we use the AV8 [11] potential, derived from the AV18 [12] by neglecting the  $(L \cdot S)$  term.

The interaction  $V_{\alpha\Lambda}$  is obtained by folding the  $\Lambda N$   $G$ -matrix interaction derived from the Nijmegen model F(NF) [13] into the density of the  $\alpha$  cluster [14], its strength being adjusted so as to reproduce the experimental value of  $B_\Lambda(^5_\Lambda\text{He})$ .

For  $V_{\Lambda N}$ , we employ effective single-channel interactions simulating the basic features of the Nijmegen model NSC97f [15], where the  $\Lambda N$ - $\Sigma N$  coupling effects are renormalized into  $\Lambda N$ - $\Lambda N$  parts: We use three-range Gaussian potentials so as to reproduce the  $\Lambda N$  scattering phase shifts calculated from the NSC97f, and then their second-range strengths in  $^3E$  and  $^1E$  states are adjusted so that calculated energies of the  $0^+-1^+$  doublet state in the  $NNN\Lambda$  four-body calculation reproduce the observed splittings of  $^4_\Lambda\text{H}$ . Furthermore, the spin-spin parts in the odd states are tuned to get the experimental values of the splitting energies of  $^7_\Lambda\text{Li}$ . The symmetric LS (SLS) and antisymmetric LS (ALS) parts in  $V_{\Lambda N}$  are chosen so as to be consistent with the  $^9_\Lambda\text{Be}$  data as follows: The SLS and ALS

parts derived from NSC97f with the  $G$ -matrix procedure are represented in the two-range form, and then the ALS part is strengthened so as to reproduce the measured  $5/2^+-3/2^+$  splitting energy with the  $2\alpha + \Lambda$  cluster model [16]. The parameters in the  $\Lambda N$  interactions are given in

$$V_{\Lambda N}(r) = \sum_{i=1}^3 \frac{1+P_r}{2} (v_0^{i,\text{even}} + \sigma_\Lambda \cdot \sigma_N v_{\sigma_\Lambda \cdot \sigma_N}^{i,\text{even}}) e^{-\beta_\Lambda^i r^2} + \frac{1-P_r}{2} (v_0^{i,\text{odd}} + \sigma_\Lambda \cdot \sigma_N v_{\sigma_\Lambda \cdot \sigma_N}^{i,\text{odd}}) e^{-\beta_\Lambda^i r^2}, \quad (3.1)$$

and listed in Table I(a).

The calculated energies of the  $0^+$  states in  $^6\text{He}$  and  $^6\text{Li}^*$  are  $-0.59$  MeV and unbounded with respect to the  $\alpha + N + N$  three-body breakup threshold, which are less bound than the observed values,  $-0.98$  MeV in  $^6\text{He}$  and  $-0.14$  MeV in  $^6\text{Li}$ . Considering that it is of vital importance in our cluster model to reproduce accurately the binding energy of all subcluster systems, we introduce an effective three-body  $\alpha NN$  interaction phenomenologically, the form of which is assumed as

$$V_{\alpha NN}(r_1, r_2) = \sum_{i=1}^2 v_i e^{-\beta^i r_1^2 - \beta^i r_2^2}, \quad (3.2)$$

where  $r_1$  and  $r_2$  are Jacobian coordinates for  $C = 1$  and  $2$  in Fig. 3 of Ref. [2].

This interaction includes four parameters  $(\beta^i, v_i)$ , which cannot be determined completely by the two binding energies of  $^6\text{He}$  and  $^6\text{Li}^*$  only. Then, the condition to reproduce the experimental value of  $^7_\Lambda\text{Li}^*$  is found to give a strong

TABLE I. (a) Parameters of the  $\Lambda N$  interaction without CSB interaction defined in Eq. (3.2). Range parameters are in  $\text{fm}^{-2}$  and the strengths are in MeV. The numbers in parentheses are even-state strengths adjusted so as to reproduce the observed spin-doublet state both in  $^4_\Lambda\text{H}$  and  $^4_\Lambda\text{He}$  with CSB interaction. (b) Parameters of the  $t(^3\text{He})\Lambda$  interaction without CSB interaction defined in Eq. (3.5). The numbers in parentheses are adjusted even-state strengths so as to reproduce the observed spin-doublet state both in  $^4_\Lambda\text{H}$  and  $^4_\Lambda\text{He}$  with CSB interaction within the framework of  $t(^3\text{He})\Lambda$  two-body model.

(a) $\Lambda N$ interaction			
$i$	1	2	3
$\beta_{\Lambda N}^i$	0.391	1.5625	8.163
$v_0^{i,\text{even}}$	-3.94	-126.1(-126.4)	1943
$v_{\sigma\sigma}^{i,\text{even}}$	-0.003	17.5(18.0)	-374.1
$v_0^{i,\text{odd}}$	-1.43	72.8	3247
$v_{\sigma\sigma}^{i,\text{odd}}$	-0.26	-61.35	-270.9
(b) $t(^3\text{He})\Lambda$ interaction			
$\mu^i$	0.2874	0.4903	0.6759
$V_0^{i,\text{even}}$	-16.37(-16.39)	-145.7(-146.1)	172.02(172.01)
$V_S^{i,\text{even}}$	0.234(0.229)	16.76(16.76)	-20.55(-20.53)
$V_0^{i,\text{odd}}$	-11.94(-11.98)	-70.27(-70.36)	679.8(678.4)
$V_S^{i,\text{odd}}$	4.525(4.537)	5.248(5.237)	-233.3(-233.8)
$\gamma^i$	0.2033	0.2033	0.2033
$\delta^i$	0.3383	0.8234	2.521
$U_0^{i,\text{even}}$	-1.995(-1.998)	-36.898(-36.99)	156.9(156.9)
$U_S^{i,\text{even}}$	0.029(0.028)	4.246(4.242)	-18.75(-18.73)
$U_0^{i,\text{odd}}$	-1.455(-1.457)	-17.791(-17.814)	620.2(618.9)
$U_S^{i,\text{odd}}$	0.552(0.553)	1.329(1.326)	-212.8(-213.3)

constraint for the parameters. The determined values of parameters are  $(\beta^1, v_1) = (0.444 \text{ fm}^{-2}, 244.8 \text{ MeV})$ ,  $(\beta^2, v_2) = (0.128 \text{ fm}^{-2}, -20.4 \text{ MeV})$ .

### B. CSB interaction

It is out of the scope of this work to explore the origin of the CSB interaction. We assume here the CSB interaction with a one-range Gaussian form

$$V_{\Lambda N}^{\text{CSB}}(r) = -\frac{\tau_z}{2} \left[ \frac{1+P_r}{2} (v_0^{\text{even,CSB}} + \sigma_\Lambda \cdot \sigma_N v_{\sigma_\Lambda \cdot \sigma_N}^{\text{even,CSB}}) e^{-\beta_{\text{even}} r^2} + \frac{1-P_r}{2} (v_0^{\text{odd,CSB}} + \sigma_\Lambda \cdot \sigma_N v_{\sigma_\Lambda \cdot \sigma_N}^{\text{odd,CSB}}) e^{-\beta_{\text{odd}} r^2} \right], \quad (3.3)$$

which includes spin-independent and spin-spin parts. In the case of the four-body calculations of  ${}^4_\Lambda\text{H}$  ( $nnp\Lambda$ ) and  ${}^4_\Lambda\text{He}$  ( $npp\Lambda$ ), the contributions of the odd-state interactions are negligibly small and their strengths cannot be determined: We take  $v_0^{\text{odd,CSB}} = 0$ , and  $v_{\sigma_\Lambda \cdot \sigma_N}^{\text{odd,CSB}} = 0$ . The range parameter,  $\beta_{\text{even}}$  is taken to be  $1.0 \text{ fm}^{-2}$ . The parameters  $v_0^{\text{even}}$  and  $v_{\sigma_\Lambda \cdot \sigma_N}^{\text{even}}$  are determined phenomenologically so as to reproduce the values of  $\Delta_{\text{CSB}}$  derived from the  $\Lambda$  binding energies of  $0^+$  and  $1^+$  states in the four-body calculation of  ${}^4_\Lambda\text{H}$  ( ${}^4_\Lambda\text{He}$ ). Then, we obtain  $v_0^{\text{even,CSB}} = 8.0 \text{ MeV}$  and  $v_{\sigma_\Lambda \cdot \sigma_N}^{\text{even,CSB}} = 0.7 \text{ MeV}$ . The calculated  $B_\Lambda$  of  $0^+$  and  $1^+$  states in  ${}^4_\Lambda\text{H}$  are  $1.99 \text{ MeV}$  and  $0.98 \text{ MeV}$ , respectively. Those in  ${}^4_\Lambda\text{He}$  are  $2.35 \text{ MeV}$  and  $1.17 \text{ MeV}$ , respectively. In these calculations, including the CSB interactions, the parameters in the CS parts are slightly modified from those in Table I(a) for fine fitting of the experimental  $B_\Lambda$  values. In Table I(a), the modified values of parameters are given in parentheses.

In order to extract the information about the odd-state part of the CSB, it is necessary to study isomultiplet hypernuclei in the  $p$ -shell region. A suitable system for such a study is  ${}^7_\Lambda\text{He}$ , in which the core nucleus  ${}^6\text{He}$  is in a bound state. (On the contrary, valence protons in  ${}^6\text{Be}$  are unbound.) Our four-body calculation for this system has to be powerful to extract the accurate information. Though there is no data about  ${}^7_\Lambda\text{He}$  at present, the coming experiments at JLAB will give us valuable data for our analyses.

Another example in the  $p$ -shell region is the isodoublet hypernuclei  ${}^8_\Lambda\text{Li}$  and  ${}^8_\Lambda\text{Be}$ , whose experimental values of  $B_\Lambda$  are obtained in emulsion. Then, it is interesting to see the contribution of the CSB interaction to the  $B_\Lambda$  values of these hypernuclei. For applications to these nuclei, we use  $\Lambda$ - $t$  and  $\Lambda$ - ${}^3\text{He}$  potentials for the CS part defined by

$$V_{\Lambda x}(\mathbf{r}, \mathbf{r}') = \sum_{i=1}^3 \frac{1}{2} \left[ (V_0^{i,\text{even}} + \mathbf{s}_\Lambda \cdot \mathbf{s}_x V_S^{i,\text{even}}) e^{-\mu^i r^2} \delta(\mathbf{r} - \mathbf{r}') + (U_0^{i,\text{even}} + \mathbf{s}_\Lambda \cdot \mathbf{s}_x U_S^{i,\text{even}}) e^{-\gamma^i (\mathbf{r}+\mathbf{r}')^2 - \delta^i (\mathbf{r}-\mathbf{r}')^2} \right] + \frac{1}{2} \left[ (V_0^{i,\text{odd}} + \mathbf{s}_\Lambda \cdot \mathbf{s}_x V_S^{i,\text{odd}}) e^{-\mu^i r^2} \delta(\mathbf{r} - \mathbf{r}') + (U_0^{i,\text{odd}} + \mathbf{s}_\Lambda \cdot \mathbf{s}_x U_S^{i,\text{odd}}) e^{-\gamma^i (\mathbf{r}+\mathbf{r}')^2 - \delta^i (\mathbf{r}-\mathbf{r}')^2} \right], \quad (3.4)$$

where  $x$  denotes  $t$  or  ${}^3\text{He}$ . The parameters are listed in Table I(b). The CSB part for  $\Lambda$ - $t$  and  $\Lambda$ - ${}^3\text{He}$  is given by

$$V_{\Lambda x}^{\text{CSB}}(\mathbf{r}, \mathbf{r}') = \frac{1}{2} \left[ (V_0^{\text{even,CSB}} + \mathbf{s}_\Lambda \cdot \mathbf{s}_x V_S^{\text{even,CSB}}) e^{-\mu_{\text{even}} r^2} \delta(\mathbf{r} - \mathbf{r}') + (U_0^{\text{even,CSB}} + \mathbf{s}_\Lambda \cdot \mathbf{s}_x U_S^{\text{even,CSB}}) e^{-\gamma_{\text{even}} (\mathbf{r}+\mathbf{r}')^2 - \delta_{\text{even}} (\mathbf{r}-\mathbf{r}')^2} \right] + \frac{1}{2} \left[ (V_0^{\text{odd,CSB}} + \mathbf{s}_\Lambda \cdot \mathbf{s}_x V_S^{\text{odd,CSB}}) e^{-\mu_{\text{odd}} r^2} \delta(\mathbf{r} - \mathbf{r}') + (U_0^{\text{odd,CSB}} + \mathbf{s}_\Lambda \cdot \mathbf{s}_x U_S^{\text{odd,CSB}}) e^{-\gamma_{\text{odd}} (\mathbf{r}+\mathbf{r}')^2 - \delta_{\text{odd}} (\mathbf{r}-\mathbf{r}')^2} \right]. \quad (3.5)$$

The parameters for even-state are adjusted so as to reproduce the data within the  $\Lambda$ - $t$  and  $\Lambda$ - ${}^3\text{He}$  cluster models for  ${}^4_\Lambda\text{H}$  and  ${}^4_\Lambda\text{He}$ , respectively. The parameters are  $V_0^{\text{even,CSB}} = 0.38 \text{ MeV}$ ,  $V_S^{\text{even,CSB}} = -0.03 \text{ MeV}$ ,  $\mu_{\text{even}} = 0.06 \text{ fm}^{-2}$ ,  $U_0^{\text{even,CSB}} = 0.08 \text{ MeV}$ ,  $U_S^{\text{even,CSB}} = -0.006 \text{ MeV}$ ,  $\gamma_{\text{even}} = 0.203 \text{ fm}^{-2}$ , and  $\delta_{\text{even}} = 0.679 \text{ fm}^{-2}$  for  ${}^8_\Lambda\text{Li}$ , and the same value with the opposite sign for  ${}^8_\Lambda\text{Be}$ . Also, as explained later, the odd-state CSB interaction is introduced phenomenologically so as to reproduce the  $B_\Lambda$  values of  ${}^8_\Lambda\text{Li}$  and  ${}^8_\Lambda\text{Be}$ . The determined parameters are  $V_0^{\text{odd,CSB}} = -0.93 \text{ MeV}$ ,  $V_S^{\text{odd,CSB}} = -0.12 \text{ MeV}$ ,  $\mu_{\text{odd}} = 0.223 \text{ fm}^{-2}$ ,  $U_0^{\text{odd,CSB}} = -0.14 \text{ MeV}$ ,  $U_S^{\text{odd,CSB}} = -0.095 \text{ MeV}$ ,  $\gamma_{\text{odd}} = 0.203 \text{ fm}^{-2}$ , and  $\delta_{\text{odd}} = 0.254 \text{ fm}^{-2}$  for  ${}^8_\Lambda\text{Li}$  and the same value with the opposite sign for  ${}^8_\Lambda\text{Be}$ . It is notable here that the odd-state CSB is of far longer range than the even-state one.

## IV. RESULTS

First, let us show the level structures of the  $T = 1$  states calculated with the  $\alpha + \Lambda + N + N$  four-body model using the same  $\Lambda N$  interaction in Ref. [4]. We calculate the bound states in those  $\Lambda$  hypernuclei.

In Figs. 2–4 and Table II, we show the level structures of  $A = 7$  hypernuclei calculated without the CSB interaction. In each figure, hypernuclear levels are shown in four columns in order to show separately the effects of even-state and odd-state  $\Lambda$ - $N$  interactions, and also the SLS and ALS interactions. Even if the CSB interactions are switched on, their small contributions do not alter the features of these figures. At first glance, the obtained  $\Lambda$  states become less bound by  $1 \text{ MeV}$  in the order of  ${}^7_\Lambda\text{He}$ ,  ${}^7_\Lambda\text{Li}^*$ , and  ${}^7_\Lambda\text{Be}$  because the repulsive Coulomb-force contributions increase in this order. In these figures, the calculated energy spectra of low-lying states of the core nuclei,  ${}^6\text{He}$ ,  ${}^6\text{Li}^*$ , and  ${}^6\text{Be}$  are also drawn in order to demonstrate the  $\Lambda$ -binding effects. Here,  ${}^6\text{He}$  and  ${}^6\text{Li}^*$  are nucleon-bound states and the  $N\alpha$  and  $NN\alpha$  interactions are adjusted so as to reproduce the observed energy spectra. Moreover,  ${}^6\text{Be}$  is a nuclear-unbound system. In order to extract the  $B_\Lambda$  value in  ${}^7_\Lambda\text{Be}$ , it is needed to subtract the total energy of the lowest  ${}^6\text{Be}$  resonant state from the calculated ground-state energy of  ${}^7_\Lambda\text{Be}$ . The energy positions of resonant states are determined by the real scaling method [17]: The obtained lowest state in  ${}^6\text{Be}$  is a  $0^+$  broad resonance, whose energy is  $0.79 \text{ MeV}$ . Thus, the experimental resonant energy  $1.37 \text{ MeV}$  cannot be reproduced when the  $\alpha N$ ,  $NN$ , and  $\alpha NN$



TABLE II. Calculated energies of the low-lying states of (a)  ${}^7_\Lambda\text{He}$ , (b)  ${}^7_\Lambda\text{Li}^*$ , and (c)  ${}^7_\Lambda\text{Be}$  without the CSB potential, together with those of the corresponding states of  ${}^6\text{He}$ ,  ${}^6\text{Li}^*$ , and  ${}^6\text{Be}$ , respectively.  $E$  stands for the total interaction energy among constituent particles. The energies in parentheses are measured from the corresponding lowest particle-decay thresholds  ${}^6_\Lambda\text{He} + N$  for  ${}^7_\Lambda\text{He}$  and  ${}^7_\Lambda\text{Li}^*$  and  ${}^5_\Lambda\text{He} + p + p$  for  ${}^7_\Lambda\text{Be}$ . The calculated rms distances,  $\bar{r}_{\alpha-N}$ ,  $\bar{r}_{\alpha-\Lambda}$  are also listed for the bound state.

(a)					
$J^\pi$	${}^6\text{He} (\alpha nn)$		${}^7_\Lambda\text{He} (\alpha nn \Lambda)$		
	$0^+$	$2^+$	$1/2^+$	$3/2^+$	$5/2^+$
$E(\text{MeV})$	-1.02	0.82	-6.39	-4.73	-4.65
$E^{\text{exp}}(\text{MeV})$	-0.98	0.83			
			(-3.10)	(-1.44)	(-1.34)
$B_\Lambda(\text{MeV})$			5.36	3.70	3.62
$B_\Lambda^{\text{exp}}(\text{MeV})$					
$\bar{r}_{\alpha-n}(\text{fm})$	4.27		3.66	3.80	3.83
$\bar{r}_{\alpha-\Lambda}(\text{fm})$			2.81	2.79	2.78
(b)					
$J^\pi$	${}^6\text{Li}^* (\alpha np)$		${}^7_\Lambda\text{Li}^* (\alpha np \Lambda)$		
	$0^+$	$2^+$	$1/2^+$	$3/2^+$	$5/2^+$
$E(\text{MeV})$	-0.12	1.77	-5.40	-3.75	-3.66
$E^{\text{exp}}(\text{MeV})$	-0.14	1.67			
			(-2.11)	(-0.46)	(-0.37)
$B_\Lambda(\text{MeV})$			5.28	3.63	3.54
$B_\Lambda^{\text{exp}}(\text{MeV})$			5.26		
$\bar{r}_{\alpha-N}(\text{fm})$	4.73		3.74	3.92	3.96
$\bar{r}_{\alpha-\Lambda}(\text{fm})$			2.82	2.80	2.80
(c)					
$J^\pi$	${}^6\text{Be} (\alpha pp)$		${}^7_\Lambda\text{Be} (\alpha pp \Lambda)$		
	$0^+$	$2^+$	$1/2^+$	$3/2^+$	$5/2^+$
$E(\text{MeV})$	0.79		-4.42		
$E^{\text{exp}}(\text{MeV})$	1.54	2.93			
			(-1.30)		
$B_\Lambda(\text{MeV})$			5.21		
$B_\Lambda^{\text{exp}}(\text{MeV})$			5.16		
$\bar{r}_{\alpha-p}(\text{fm})$			3.84		
$\bar{r}_{\alpha-\Lambda}(\text{fm})$			2.83		

interactions are adopted so as to reproduce the bound-state energies of  ${}^6\text{He}$  and  ${}^6\text{Li}^*$ .

It is particularly interesting to see the glue-like role of the  $\Lambda$  particle in  $A = 7$  hypernuclear systems. Though the ground state of  ${}^6\text{Be}$  is unbound, the  $\Lambda$  participation leads to a bound state below the lowest  ${}^5_\Lambda\text{He} + p + p$  threshold, the binding energy of which is about 1.3 MeV. The ground states of the core nuclei  ${}^6\text{He}$  and  ${}^6\text{Li}^*$  are weakly bound by 1.02 and 0.12 MeV below the  $\alpha + N + N$  threshold. Owing to an additional  $\Lambda$  particle, those of  ${}^7_\Lambda\text{He}$  and  ${}^7_\Lambda\text{Li}^*$  become rather deeply bound by about 2 ~ 3 MeV below the respective lowest thresholds. It should be noted here that the calculated values of  $B_\Lambda$  of  ${}^7_\Lambda\text{Li}^*$  and  ${}^7_\Lambda\text{Be}$  are in good agreement with the experimental values, as shown in Table II. The  $5/2^+$  and  $3/2^+$  excited states in  ${}^7_\Lambda\text{Li}^*$

are predicted to be in weakly bound states with respect to the  ${}^6_\Lambda\text{He} + p$  threshold. Furthermore, the corresponding states in  ${}^7_\Lambda\text{He}$  are in deeper bound states by about 1.3 MeV with respect to the  ${}^6_\Lambda\text{He} + n$  threshold. This difference is due to the  $\alpha p$  Coulomb repulsion in the former not being active in the latter.

In the past calculation [2], the uppermost bound states in  ${}^7_\Lambda\text{He}$ ,  ${}^7_\Lambda\text{Li}^*$ , and  ${}^7_\Lambda\text{Be}$  were  $5/2^+$ ,  $3/2^+$ , and  $1/2^+$  states, respectively. These states are very weakly bound structures and exhibit halo or skin structures having long tails in density distributions of valence nucleons. In comparison with these calculations, performed in the limited three-body model space ( ${}^5_\Lambda\text{He} + N + N$ ), all states in  $A = 7$  systems become more deeply bound in the present four-body model. This tendency is reasonable because, in the present calculations, the excitation effects of a  $\Lambda$  particle are fully taken into account in the treatment with use of the  $\Lambda N$  effective interactions chosen consistently with the four-body model space. It is instructive to compare the tail behavior of the density distributions of valence nucleons in the four-body model with those in the three-body model. We derive here the nucleon density distributions of  $5/2^+$  states in  ${}^7_\Lambda\text{He}$  and  ${}^7_\Lambda\text{Li}$  and that of  $1/2^+$  state in  ${}^7_\Lambda\text{Be}$  using the two models.

In Table II, we list the calculated values of the root mean square (rms) radii between  $\alpha$  and  $N$  ( $\bar{r}_{\alpha-N}$ ) and those between  $\alpha$  and  $\Lambda$  ( $\bar{r}_{\alpha-\Lambda}$ ) in our four-body models of  ${}^7_\Lambda\text{He}$ ,  ${}^7_\Lambda\text{Li}^*$ , and  ${}^7_\Lambda\text{Be}$ . As shown here, the values of  $\bar{r}_{\alpha-n}$  in these systems are larger than those of  $\bar{r}_{\alpha-\Lambda}$ , indicating that the distributions of valence nucleons are of longer-ranged tails than those of the  $\Lambda$ 's in the respective systems. However, all rms radii in the four-body models are shorter than those in the three-body models [2], that is, the four-body binding energies in the present model are larger than the three-body ones in the previous model. This means that the distributions of nucleons and  $\Lambda$  around  $\alpha$  obtained in the four-body models are more compact than those in the three-body models.

In order to see the structures of these systems visually, in Fig. 5 we draw the density distributions of  $\Lambda$  (dashed curve) and valence neutrons (solid curve) of the  $5/2^+$  states in  ${}^7_\Lambda\text{He}$  and  ${}^7_\Lambda\text{Li}^*$  and of the  $1/2^+$  state in  ${}^7_\Lambda\text{Be}$ . For comparison here, also a single-nucleon density in the  $\alpha$  core is shown by the dotted curve. In each case, the density distribution of the  $\Lambda$  has a shorter-ranged tail than that of the two valence nucleons, but is extended significantly far away from the  $\alpha$  core. This structure can be nicely imaged as three layers of matter distribution composed of an  $\alpha$  core, a  $\Lambda$  skin, and a neutron (proton) halo. Here, the proton-density distribution in the  $5/2^+$  state of  ${}^7_\Lambda\text{Li}^*$  has a particularly longer tail than those in the others due to the very weak binding of the halo proton from the lowest  ${}^6_\Lambda\text{He} + p$  threshold.

It is considered that the  $3/2^+ - 5/2^+$  spin-doublet states in  ${}^7_\Lambda\text{He}$  and  ${}^7_\Lambda\text{Li}^*$  give valuable information about the underlying spin-dependence of the  $\Lambda N$  interaction. Let us investigate these states straightforwardly with use of the  $\Lambda N$  interaction determined in the analysis for the  $T = 0$  spin-doublet states in  ${}^7_\Lambda\text{Li}$ . The results for  ${}^7_\Lambda\text{He}$  and  ${}^7_\Lambda\text{Li}^*$  are displayed in Figs. 2 and 3, respectively. Because their features are not different from each other, here we pick up the former case.

Then, let us remark how the energies of the  $3/2^+ - 5/2^+$  spin-doublet states are changed by adding the components

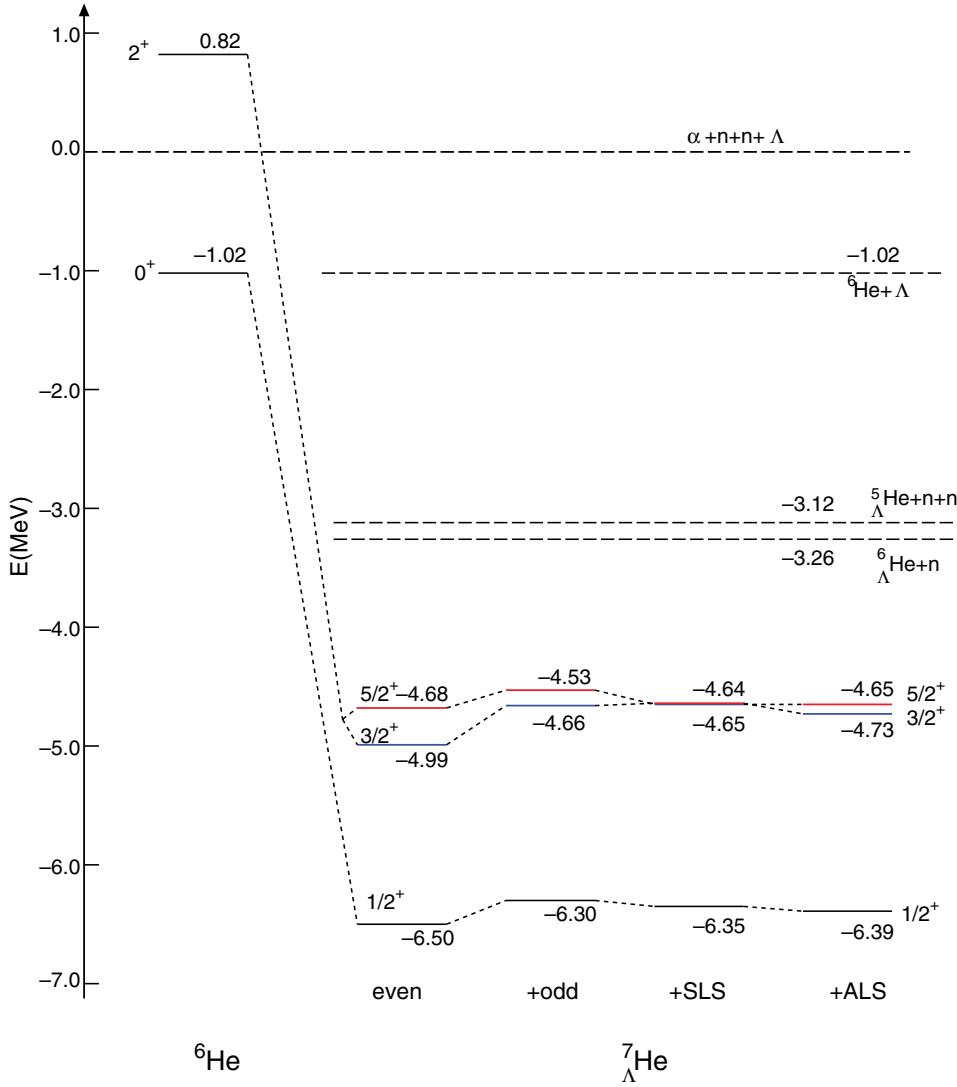


FIG. 2. (Color online) Calculated energy levels of  ${}^6\text{He}$  and  ${}^7\text{He}$ . The CSB potential is not included in  ${}^7_\Lambda\text{He}$ . The level energies are measured from the particle breakup threshold.

of  $\Lambda N$  interaction successively. We see that the resultant energy splitting of  $5/2^+-3/2^+$  states in  ${}^7_\Lambda\text{He}$  is given as about 0.1 MeV, being the combined contributions from the spin-spin, SLS, and ALS interactions as explained in the following. We can see the same tendency in  ${}^7_\Lambda\text{Li}^*$  in Fig. 3.

It should be noted here that the splitting energies of the  $T = 1$   $3/2^+-5/2^+$  states are much smaller than those of the  $T = 0$   $1/2^+-3/2^+$  and  $5/2^+-7/2^+$  doublet states in  ${}^7_\Lambda\text{Li}$  given in Ref. [2]. To understand the reason for the difference between the  $T = 1$  and  $T = 0$  doublet splittings, we remark that the spin-isospin structure of  $NN\Lambda$  system on the  $\alpha$  core is  $[(NN)_{sTT_c}\Lambda]_s$  [cf. Eq. (2.3)]. In the case of the  $T = 1$  states, the corresponding  $nn$  pair is in spin-singlet states ( $s = 0$ , spin antiparallel), while in  ${}^7_\Lambda\text{Li}$  ( $T = 0$ ) the  $np$  pair outside the  $\alpha$  core is in a spin-triplet state ( $s = 1$ , spin-parallel). In general the numbers of  $\Lambda N$  triplet and singlet bonds are different between the  $J_>$  and  $J_<$  partner states. Thus, the difference in the spin-value of  $(NN)_{s=1\text{or}0}$  leads to the different contributions of the  $\Lambda N$  spin-spin interactions to the doublet splittings. Let us see in more detail how the  $\Lambda N$

spin-spin interactions contribute to the  $3/2^+-5/2^+$  splitting in  ${}^7_\Lambda\text{He}$  ( $T = 1$ ). Both doublet states are composed of the  $L = 2$   $(nn)_{s=0,T=1}$  pair in the spin-singlet state coupled to the  $s$ -state  $\Lambda$ . As mentioned previously, the situation is notably different from that of the  $5/2^+-7/2^+$  doublet in  ${}^7_\Lambda\text{Li}$  ( $T = 0$ ) which is based on the  $[L = 2 (pn)_{s=1,T=0}]_{J=3^+}$  core state, and therefore, the  $J_> = 7/2^+$  partner is characterized by the spin-stretched configuration. In contrast to the  $T = 0$  case, both of the  $J_< = 3/2^+$  state and the  $J_> = 5/2^+$  state in  ${}^7_\Lambda\text{He}$  ( $T = 1$ ) include  $\Lambda N$  spin-singlet and spin-triplet states. However, we find that the contribution of the  $\Lambda N$  spin-singlet state is negligibly small in the  $J_> = 5/2^+$  state. As a result, the even-state spin-spin part of the  $\Lambda N$  interaction gives rise to the splitting energy of about 0.31 MeV (see “even” column). In addition, when the odd-state interaction is switched on, the energy splitting is reduced to be about 0.13 MeV (see “+odd” column). The major reason for this reduction is because  $V_{\Lambda N}^{(1O)}$  is more repulsive than  $V_{\Lambda N}^{(3O)}$ , and therefore, the  $3/2^+$  state including  $\Lambda N$  spin-singlet component is pushed up more than the  $5/2^+$  state.

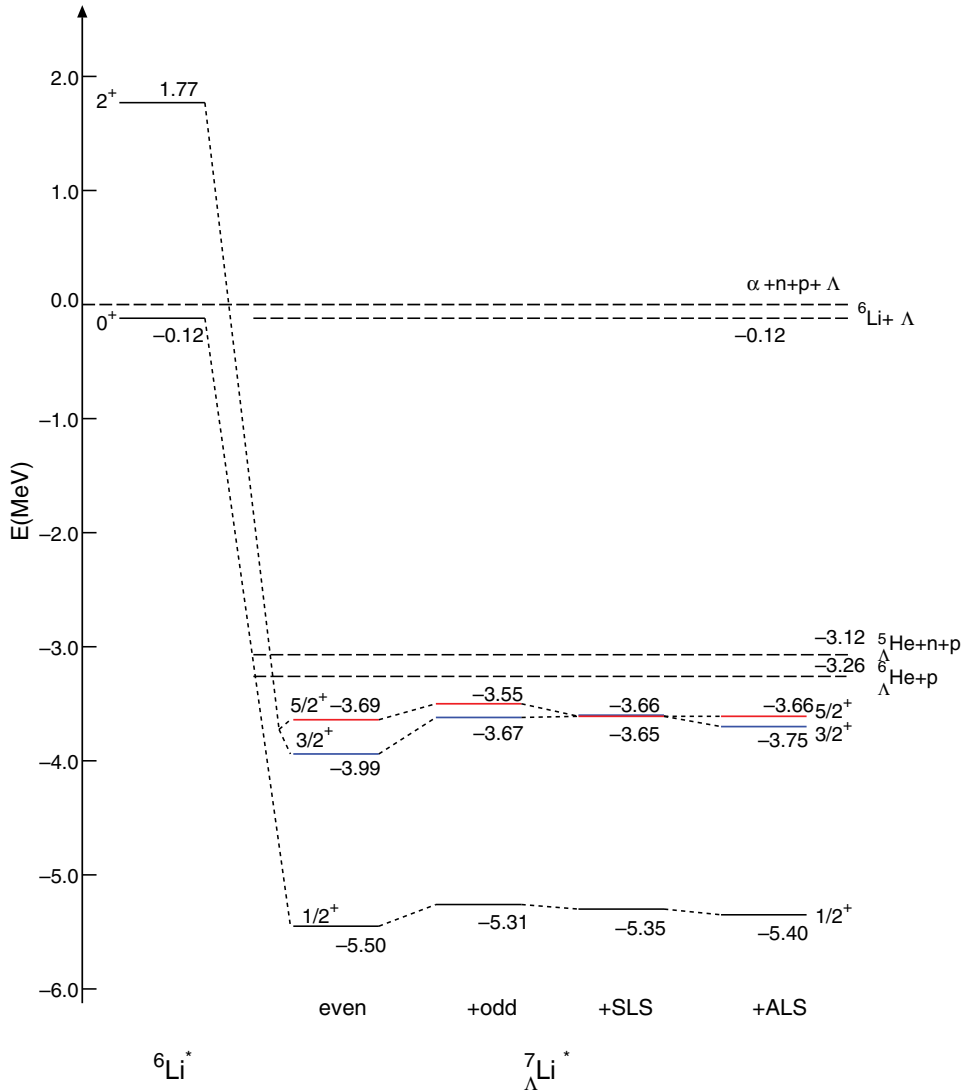


FIG. 3. (Color online) Calculated energy levels of  ${}^6\text{Li}^*$  and  ${}^7_\Lambda\text{Li}^*$ . The CSB potential is not included in  ${}^7_\Lambda\text{Li}^*$ . The level energies are measured from the particle breakup threshold.

Moreover, we continue to add SLS and ALS contributions to the  $3/2^+$  and  $5/2^+$  doublet states. As shown in Fig. 2, the SLS works attractively for the  $5/2^+$  state because the contribution of the  $\Lambda N$  spin-triplet state is dominated in this state. Furthermore, the ALS works significantly in the  $3/2^+$  state because the ALS acts between the spin = 0 and 1  $\Lambda N$  states. However, the ALS does not efficiently work in the  $5/2^+$  state because the spin-singlet component is small in this state. As a result, the energy splitting of the  $5/2^+$ - $3/2^+$  states including both the spin-spin and spin-orbit terms in  ${}^7\text{He}$  leads to 0.08 MeV. We can see the same tendency in  ${}^7_\Lambda\text{Li}^*$  and the resultant splitting is 0.09 MeV, as shown in Fig. 3. If the experimental energy resolution becomes good enough to discuss the present splitting energy, we will have a chance of getting information about the spin-dependent parts of the  $\Lambda N$  interaction.

There still remain certain effects of the  $\Lambda N$  tensor interaction on the doublet splittings. In this article, for the  $T = 1$  isotriplet states ( $A = 7$ ), however, we apply the prescription adopted in the analysis of the  $T = 0$   ${}^7_\Lambda\text{Li}$  states [4], and therefore, we do not include the tensor component. Here, we note that the  $\Lambda N$ - $\Lambda N$  tensor contribution is small compared to

the spin-spin interaction, however, another tensor effect comes from the  $\Lambda N$ - $\Sigma N$  coupling. In fact, accounting for the  $\Sigma$ - $\Lambda$  coupling by modifying the  $\Lambda N$  interaction alters its effect on doublet splitting, and hence introduces an uncertainty in the calculation. According to the  $\Sigma$ -mixing studied within the shell model [18], the energy shifts amount to several tens of keV in some of the  $T = 0$  states of  ${}^7_\Lambda\text{Li}$ . The cluster model estimates for such effects will be discussed in the next stage.

## V. CHARGE SYMMETRY BREAKING EFFECTS

### A. CSB effects in $A = 7$ four-body models

Let us focus on the ground states in  ${}^7_\Lambda\text{He}$  and  ${}^7_\Lambda\text{Be}$  and the  $T = 1$   $1/2^+$  state in  ${}^7_\Lambda\text{Li}$ , which are the members of the isotriplet. The CSB effect has to be reflected also in their binding energies in the same way as in the  $T = 1/2$  isodoublet members  ${}^4_\Lambda\text{H}$  and  ${}^4_\Lambda\text{He}$ .

As explained in Sec. III B, we introduce the phenomenological CSB potential with the central-force component only. The CS part of the two-body  $\Lambda N$  interaction is fixed to reproduce the averaged energy spectra of  ${}^4_\Lambda\text{H}$  and  ${}^4_\Lambda\text{He}$ , and then the CSB

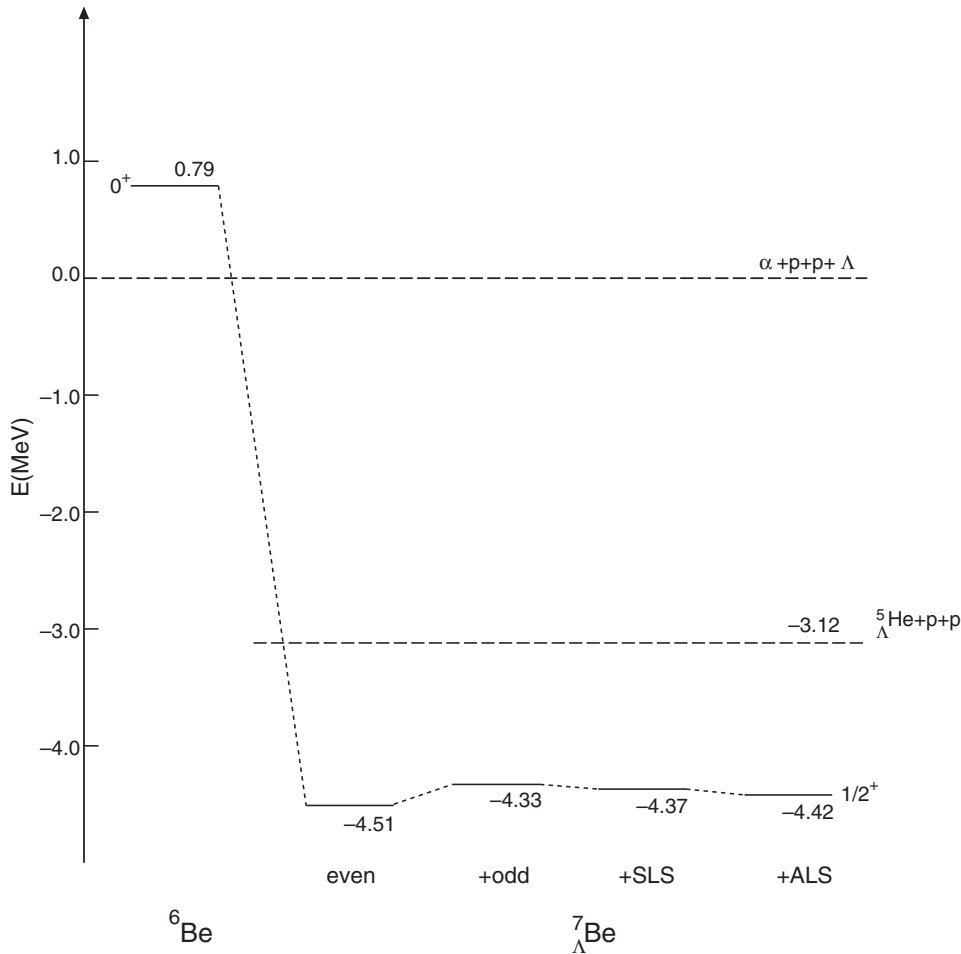


FIG. 4. Calculated energy levels of  ${}^6\text{Be}$  and  ${}^7_{\Lambda}\text{Be}$ . The CSB potential is not included in  ${}^7_{\Lambda}\text{Be}$ . The level energies are measured from the particle breakup threshold.

part is adjusted so as to reproduce simultaneously the energy levels of these hypernuclei. The spin-spin part of the CSB can be determined by performing this by adjusting the procedures both for the  $0^+$  and  $1^+$  states.

First, in Fig. 6, we show the energy spectra of  $A = 7$  hypernuclei without the CSB interaction. The ground-state energy of  ${}^7_{\Lambda}\text{He}$  is  $-6.39$  MeV with respect to the  $\alpha + n + n + \Lambda$  four-body breakup threshold. With the increase of the proton numbers, the Coulomb repulsion becomes more and more effective in going from  ${}^7_{\Lambda}\text{Li}^*$  to  ${}^7_{\Lambda}\text{Be}$ . Recently, in the KEK-E419 experiment [3], the  $T = 1$   $1/2^+$  state of  ${}^7_{\Lambda}\text{Li}$  was produced. The observed value of  $B_{\Lambda} = 5.26$  MeV is in good agreement with our calculated value of 5.28 MeV. In the case of  ${}^7_{\Lambda}\text{Be}$ , there are the old emulsion data giving  $B_{\Lambda} = 5.16$  MeV. This value should be compared with our obtained value of 5.21 MeV. Then, the  $B_{\Lambda}$  value in the ground  $1/2^+$  state of  ${}^7_{\Lambda}\text{He}$  is predicted to be 5.36 MeV without taking the CSB effect into account.

Next, let us consider the CSB effects in  $A = 7$  isotriplet hypernuclei. In Fig. 7, we show the energy spectra of those hypernuclei calculated with the CSB interaction switched on. In the  ${}^7_{\Lambda}\text{Li}$  case, the CSB interaction brings about almost no contribution to the  $\Lambda$  binding energies because there is one proton and one neutron outside the  $\alpha$  core and the  $\Lambda n$  and  $\Lambda p$  CSB interactions cancel each other out. Furthermore, the CSB interaction works repulsively (+0.20 MeV) and attrac-

tively ( $-0.20$  MeV) in the  ${}^7_{\Lambda}\text{He}$  and  ${}^7_{\Lambda}\text{Be}$  cases, respectively. Therefore, our result indicates that, if the experimental energy resolution is as good enough as less than 0.2 MeV, the CSB effect can be observed in these cases. It should be noted here that only the even-state part of our CSB interaction is taken into account in being consistent with the observed binding energies of  ${}^4_{\Lambda}\text{H}$  and  ${}^4_{\Lambda}\text{He}$ .

In the  ${}^7_{\Lambda}\text{Be}$  case, the  $\Lambda$  energy becomes more bound by 0.2 MeV due to the attractive CSB interaction between the  $\Lambda$  and two protons, that is,  $B_{\Lambda} = 5.44$  MeV. The experimental  $B_{\Lambda}$  value is found to be reproduced without the CSB effect and the inclusion of the CSB contribution goes unfavorably. In order to reproduce the binding energy of  ${}^7_{\Lambda}\text{Be}$ , the CSB interaction seems to be vanishing or even of opposite sign from that in the  $A = 4$  system. There still remains a problem in our treatment for the  ${}^7_{\Lambda}\text{Be}$  system: The calculated value of 0.79 MeV of the lowest resonance energy of the  ${}^6\text{Be}$  is not in agreement with the experimental value of 1.37 MeV. When the attractive  $\alpha pp$  interaction is switched off, the  ${}^6\text{Be}(0^+)$  resonance energy becomes 1.18 MeV, which is still a bit lower than the observed value. This change of the calculated resonance energy from 0.79 to 1.18 MeV makes the  $B_{\Lambda}$  value smaller by only 30 keV. Thus, the change of the  $B_{\Lambda}$  value is considered to be so small, even if the  $\alpha pp$  interaction is adjusted so as to just reproduce the value of 1.37 MeV.



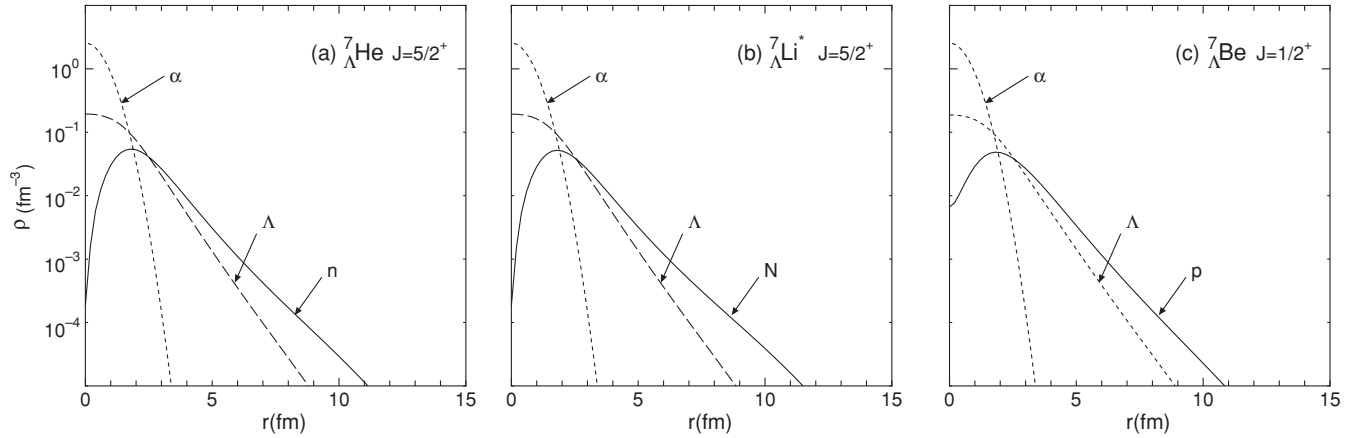


FIG. 5. Calculated density distribution of  $\alpha$ ,  $\Lambda$ , and valence nucleons for (a)  ${}^7_{\Lambda}\text{He}$ , (b)  ${}^7_{\Lambda}\text{Li}^*$ , and (c)  ${}^7_{\Lambda}\text{Be}$  without charge symmetry breaking potential.

In the  ${}^7_{\Lambda}\text{He}$  case, the CSB interaction between the  $\Lambda$  and two valence neutrons works repulsively and the ground-state binding energy becomes  $B_{\Lambda} = 5.16$  MeV, less bound by 0.2 MeV, than the value without the CSB effect. Though there is no data for  ${}^7_{\Lambda}\text{He}$  at present, the  $B_{\Lambda}$  of  ${}^7_{\Lambda}\text{He}$  will be obtained soon by the  $(e, e'K^+)$  reaction experiment done at JLAB. It is interesting to know whether or not the CSB effect in  ${}^7_{\Lambda}\text{He}$  is consistent with the emulsion data for  $B_{\Lambda}({}^7_{\Lambda}\text{Be})$ .

### B. CSB effects in $A = 8$ cluster models

Let us study another set of two mirror hypernuclei,  ${}^8_{\Lambda}\text{Li}$  and  ${}^8_{\Lambda}\text{Be}$ , in the  $p$ -shell region within the framework of the  $\alpha t\Lambda$  and  $\alpha^3\text{He}\Lambda$  cluster models.

The experimental values of  $B_{\Lambda}$  from the emulsion data are  $6.80 \pm 0.03$  MeV and  $6.84 \pm 0.05$  MeV for  ${}^8_{\Lambda}\text{Li}$  and  ${}^8_{\Lambda}\text{Be}$ , respectively. Thus, the energy difference  $\Delta B_{\Lambda}^{(8)} = B_{\Lambda}({}^8_{\Lambda}\text{Be}) - B_{\Lambda}({}^8_{\Lambda}\text{Li})$  is 0.04 MeV, which is much

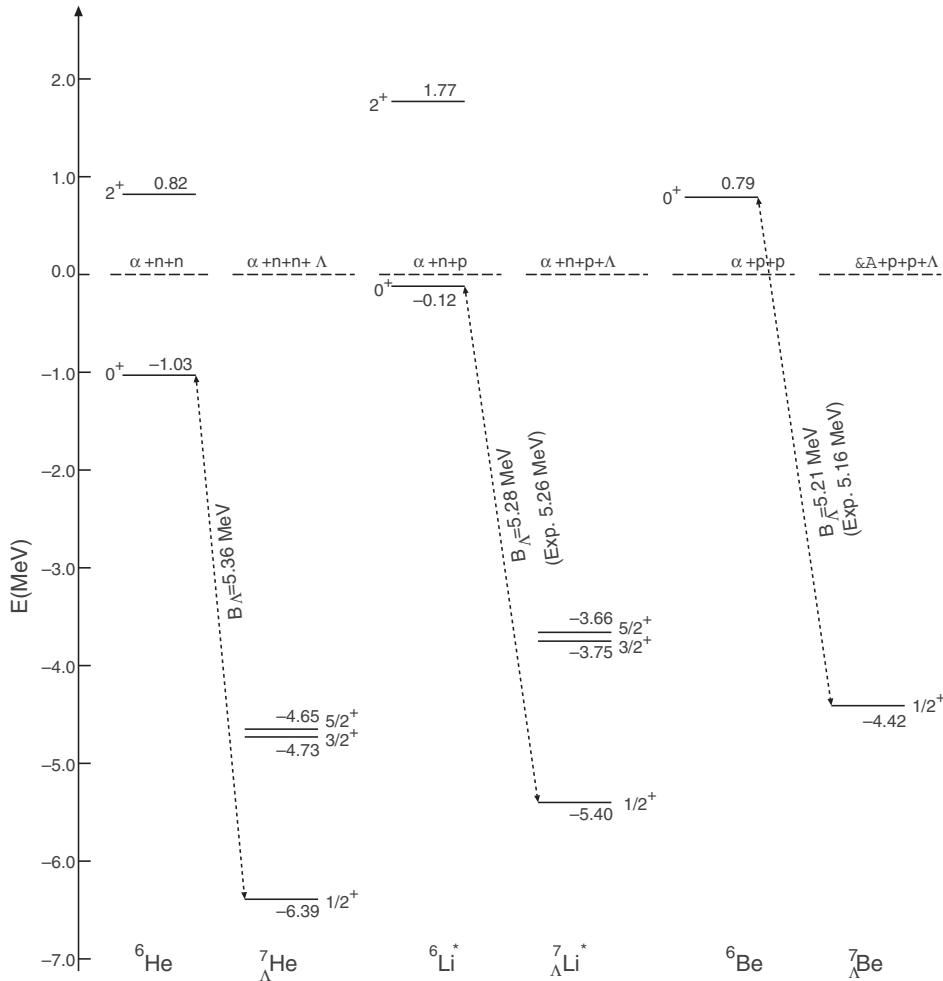


FIG. 6. The calculated energy levels of  ${}^6\text{He}$ ,  ${}^7_{\Lambda}\text{He}$ ,  ${}^6\text{Li}^*$ ,  ${}^7_{\Lambda}\text{Li}^*$ ,  ${}^6\text{Be}$ , and  ${}^7_{\Lambda}\text{Be}$  with spin-spin and spin-orbit  $\Lambda N$  interactions. The CSB potential is not included in the calculated energies of  $A = 7$  hypernuclei. The energies are measured from the particle breakup threshold.

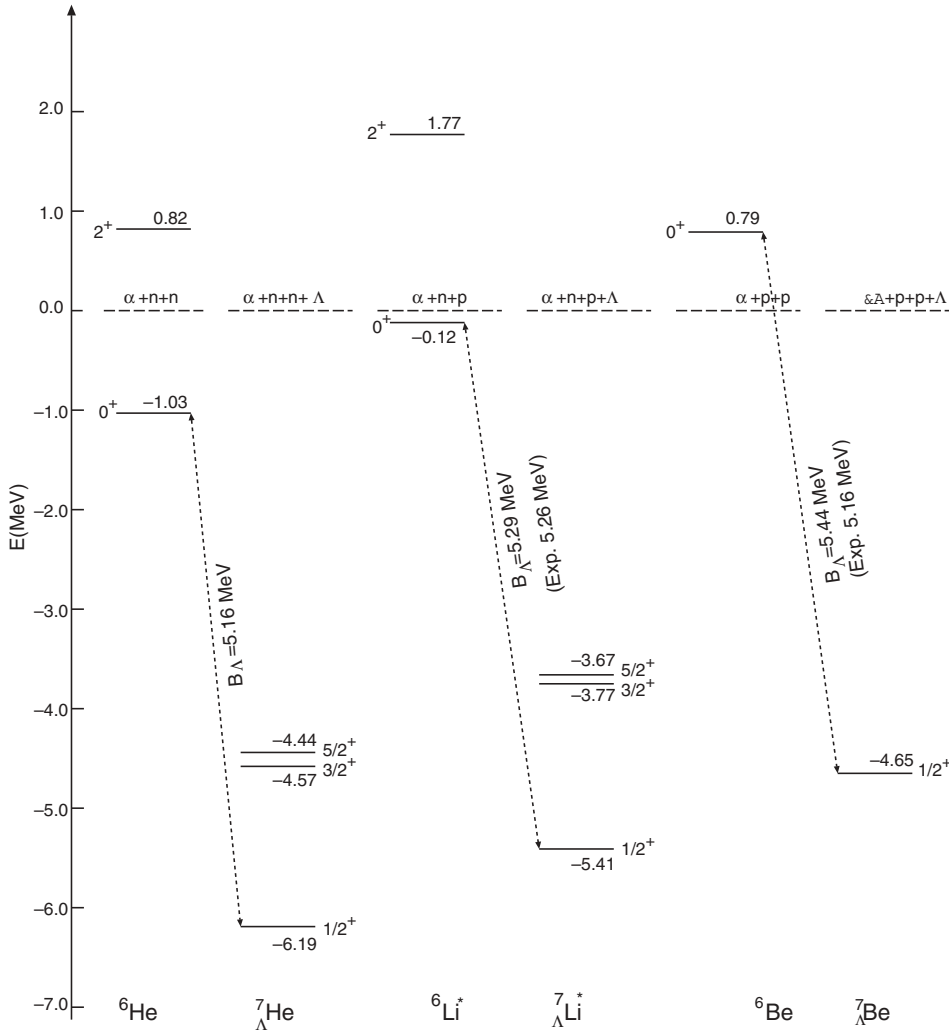


FIG. 7. The calculated energy levels of  ${}^6\text{He}$ ,  ${}^7\text{He}$ ,  ${}^6\text{Li}^*$ ,  ${}^7\text{Li}^*$ ,  ${}^6\text{Be}$ , and  ${}^7\text{Be}$  with spin-spin and spin-orbit  $\Lambda N$  interactions. The charge symmetry breaking potential is included in the calculated energies of  $A = 7$  hypernuclei. The energies are measured from the particle breakup threshold.

smaller than the experimental value of  $\Delta B_\Lambda^{(4)} = B_\Lambda({}^4\text{He}) - B_\Lambda({}^4\text{H}) = 0.35$  MeV. It was pointed out Ref. [6] that, due to the strong Coulomb force in  $A = 8$  hypernuclei,  $\Delta B_\Lambda^{(8)}$  seems small and hence the charge symmetry breaking effect seems small. It is interesting to see how much  $\Delta B_\Lambda^{(8)}$  is obtained in an actual microscopic calculation by introducing the phenomenological CSB interaction.

In our previous work [2], the cluster model calculations were performed for these hypernuclei with use of the charge symmetric  $\alpha$ - $t$ ( ${}^3\text{He}$ ),  $\Lambda$ - $\alpha$ , and  $\Lambda$ - $t$ ( ${}^3\text{He}$ ) interactions adjusted so as to reproduce the experimental value 6.80 MeV for  ${}^8_\Lambda\text{Li}$ . Then, the obtained value of  $B_\Lambda$  was 6.72 MeV for  ${}^8_\Lambda\text{Be}$ , where the difference from the value for  ${}^8_\Lambda\text{Li}$  was only due to the difference of the Coulomb-force contributions.

In order to see the effect of the CSB interaction, we repeat the energy level calculations employing the present interactions given in Sec. III. When only the CS parts of  $\Lambda N$  interactions are used, the calculated values of  $B_\Lambda({}^8_\Lambda\text{Li})$  and  $B_\Lambda({}^8_\Lambda\text{Be})$  are 6.80 and 6.84 MeV, respectively. Here, these CS parts are slightly modified from that in Ref. [19] so as to reproduce well the experimental value of  $B_\Lambda({}^8_\Lambda\text{Li})$  finally. Switching on the CSB parts, the calculated values of  $B_\Lambda$  become 6.74 and 6.90 MeV for  ${}^8_\Lambda\text{Li}$  and  ${}^8_\Lambda\text{Be}$ , respectively.

Then, the calculated value of  $\Delta B_\Lambda^{(8)} = B_\Lambda({}^8_\Lambda\text{Be}) - B_\Lambda({}^8_\Lambda\text{Li})$  is 0.16 MeV. Thus, the use of the CSB interaction determined in the  $A = 4$  systems leads to a larger value of  $\Delta B_\Lambda^{(8)}$  in comparison with the experimental value of 0.04 MeV. In order to reproduce the experimental value of  $\Delta B_\Lambda^{(8)}$ , here, let us try introducing an odd-state CSB interaction phenomenologically, whose contributions in the  $A = 4$  systems are negligible: We find that the experimental values of  $B_\Lambda$  for  ${}^8_\Lambda\text{Li}$  and  ${}^8_\Lambda\text{Be}$  can be reproduced by adding a rather long-ranged odd-state interaction with the opposite sign of the even state CSB interaction described in Eq. (3.5). The  $B_\Lambda$  values of  ${}^8_\Lambda\text{Li}$  and  ${}^8_\Lambda\text{Be}$ , calculated with both even-state and odd-state CSB interactions, are 6.81 MeV and 6.83 MeV, respectively, which are in good agreement with the data.

The present framework for the  $A = 8$  isomultiplet systems has a sort of limitation in the sense that the  $t$ ( ${}^3\text{He}$ ) cluster is assumed to have three nucleons of the same size of those in  $\alpha$ . However, the results for both systems of  $A = 7$  and 8 are qualitatively consistent with each other, and the odd state of the CSB interaction are found to have an opposite sign of the even state CSB interaction determined at  $A = 4$  hypernuclei.

In the near future, we expect to have the observed  $B_\Lambda$  of  ${}^7_\Lambda\text{He}$  from the  $(e, e'K^+)$  reaction experiment done at JLAB. On the basis of the coming data, it might be possible to get information on the odd-state CBS interactions. Another example to clarify the even-state and odd-state CSB interactions is to study  ${}^{10}_\Lambda\text{Be}$  with an  $\alpha\alpha N\Lambda$  four-body model. This four-body calculation is in progress. Also, we hope to observe the  $B_\Lambda$  of this hypernucleus by  ${}^{10}\text{B}(e, e'K^+){}^{10}_\Lambda\text{Be}$  at JLAB in the future.

## VI. SUMMARY

We study the structures of the  $T = 1$  triplet hypernuclei ( ${}^7_\Lambda\text{He}$ ,  ${}^7_\Lambda\text{Li}$ , and  ${}^7_\Lambda\text{Be}$ ) within the framework of  $\alpha + \Lambda + N + N$  four-body model. In the previous article, this four-body model proved to work successfully in the detailed analysis of the  $T = 0$  energy levels of  ${}^7_\Lambda\text{Li}$ , which are best known through the high-resolution  $\gamma$ -ray measurements. The present framework is also a natural extension of the previous calculations performed with the  ${}^5_\Lambda\text{He} + N + N$  three-body model in which the  $\Lambda$  particle motion was confined to form the  ${}^5_\Lambda\text{He}$  ground state.

The major conclusions are summarized as follows:

- (i) On the basis of reasonable  $\alpha p(n)$ ,  $\alpha pn$ ,  $\alpha\Lambda$ , and  $N\Lambda$  interactions, which well describe the binding energies of all subcluster units ( $\alpha pn$ ,  $\alpha\Lambda$ , and  $N\Lambda$ ), we make extensive and successful structure analyses for the  $T = 1$  states of  $A = 7$  isotriplet hypernuclei. One of the nontrivial and important outcomes is that the observed  $B_\Lambda$  value of the  $T = 11/2^+$  state in  ${}^7_\Lambda\text{Li}$  is reproduced nicely with the use of the  $\alpha\Lambda$  and  $\Lambda N$  interactions determined in  $T = 0$  states of  ${}^7_\Lambda\text{Li}$ . Also the  $B_\Lambda({}^7_\Lambda\text{Be})$  observed in emulsion is reproduced well, though there still remains a problem that the unbound  ${}^6\text{Be } 0^+$  state is calculated at a bit lower position in comparison with the observed resonance energy. The  $\Lambda$  binding energy for  ${}^7_\Lambda\text{He}$  ( $J = 1/2^+$ ), which is not observed so far, is calculated to be around 5.16–5.36 MeV (with or without the CSB interaction). This result will be tested when the result of the  ${}^7\text{Li}(e, e'K^+){}^7_\Lambda\text{He}$  experiment comes from JLAB.
- (ii) As one of the purposes of the extended calculations, we carefully test whether the  $3/2^+$  and  $5/2^+$  spin-doublet excited states ( $s_{1/2}$   $\Lambda$  coupled to the  $2^+$  excited core) are bound or not, since they were calculated previously to be just above the nucleon breakup threshold (weakly unbound) as a result of the limited three-body model of  ${}^5_\Lambda\text{He} + N + N$ . It is interesting to see the glue-like role of the  $\Lambda$  particle carefully when it is added to the core nuclei having a nucleon halo structure, as concerned here. In this article, the four-body calculation, which allows free motion of  $\Lambda$ , gives a clear prediction that the excited spin-doublet states in  ${}^7_\Lambda\text{He}$  ( ${}^7_\Lambda\text{Li}$ ) become bound, respectively, at 1.3 MeV (0.3 MeV) below the lowest nucleon-breakup threshold  ${}^6_\Lambda\text{He} + n$  ( ${}^6_\Lambda\text{He} + p$ ). The energy splitting between these  $T = 1$  doublet states comes from the spin-spin and spin-orbit interactions, which is calculated to be around 0.1 MeV. If any coincidence experiment is available, and the energy resolution

is good enough to resolve the 0.1 MeV splitting, one will have a chance of extracting information on the spin-dependent interactions. In  ${}^7_\Lambda\text{Be}$ , however, we do not expect to get the corresponding bound excited states.

- (iii) It is interesting to get the three-layer structure of the matter distributions in the  $T = 1$  isotriplet hypernuclear states, which consist of the  $\Lambda$  particle coupled to the nuclear core having a neutron or proton halo. The typical numbers of the rms radii for the  ${}^7_\Lambda\text{He}$  ( $J = 5/2^+$ ),  ${}^7_\Lambda\text{Li}^*$  ( $J = 5/2^+$ ) and  ${}^7_\Lambda\text{Be}$  ( $J = 1/2^+$ ) states are calculated to be  $\bar{r}_\alpha = 1.4$  fm for innermost  $\alpha$ ,  $\bar{r}_{\alpha-\Lambda} = 2.8$  fm for the  $\Lambda$  distribution, and  $\bar{r}_{\alpha-n} = 3.8$  fm for the outermost valence nucleon distribution.
- (iv) The charge symmetry breaking effects in light  $p$ -shell hypernuclei are investigated quantitatively for the first time on the basis of the phenomenological CSB interaction, which describe the experimental energy difference between  $B_\Lambda({}^4_\Lambda\text{H})$  and  $B_\Lambda({}^4_\Lambda\text{He})$ . Here, we find that the inclusion of this CSB interaction gives rise to push up the  ${}^7_\Lambda\text{He}$  energy by 0.20 MeV, but it pushes down the  ${}^7_\Lambda\text{Be}$  energy by 0.20 MeV. In  ${}^7_\Lambda\text{Li}^*$ , the level energies remain unchanged by adding the CSB interaction due to cancellation between the contribution of valence proton and neutron on  $\alpha$ . Comparing the calculated value of  $B_\Lambda({}^7_\Lambda\text{Be})$  with the emulsion data, it seems that the CSB interaction makes the agreement worse. In the case of  ${}^7_\Lambda\text{Be}$ , however, there remains the problem of treating the unbound  ${}^6\text{Be}$  core within our framework. The CSB effect is expected to appear more clearly in the coming data of  ${}^7_\Lambda\text{He}$  whose core nucleus  ${}^6\text{He}$  is a bound system. Next, we try to explain the binding energy difference of the  $T = 1/2$  isodoublet  $A = 8$  hypernuclei ( ${}^8_\Lambda\text{Li}$ ,  ${}^8_\Lambda\text{Be}$ ), adopting the phenomenological three-body models of  $\alpha + t + \Lambda$  and  $\alpha + {}^3\text{He} + \Lambda$ , respectively. The energy difference between  ${}^8_\Lambda\text{Li}$  and  ${}^8_\Lambda\text{Be}$ , obtained in emulsion, cannot be reproduced accurately with the use of our CSB interaction. Thus, our analyses for  $p$ -shell hypernuclei demonstrate that the CSB interaction determined in the  ${}^4_\Lambda\text{H}$  and  ${}^4_\Lambda\text{He}$  doublet is not necessarily consistent with the experimental  $B_\Lambda$  values of  ${}^7_\Lambda\text{Be}$ ,  ${}^8_\Lambda\text{Li}$ , and  ${}^8_\Lambda\text{Be}$  in emulsion.
- (v) As a trial, we introduce the odd-state component of the CSB interaction, which is of a longer range than the even-state one. In order to reproduce the experimental data of  ${}^8_\Lambda\text{Li}$  and  ${}^8_\Lambda\text{Be}$ , it is found to be necessary that the sign of the odd-state part is opposite to that of the even part. It is likely that such an odd-state CSB interaction plays some role in the above  $A = 7$  four-body systems.

It is known that the CSB are generated essentially by the mass difference within the  $\Sigma$ -multiplet mixed, and the  $\Lambda - \Sigma^0$  mixing in the meson-theoretical model. Thus, in order to get a firm conclusion on this matter, it is necessary to perform a four-body calculation of  $A = 4$   $\Lambda$  hypernuclei and  $A = 7$   $\Lambda$  hypernuclei taking  $NNN\Lambda$  and  $NNN\Sigma$ , and  $\alpha\Lambda NN$  and  $\alpha\Sigma NN$ , respectively. These types of calculations are in progress.

## ACKNOWLEDGMENTS

The authors thank Professors O. Hashimoto, H. Tamura, B. F. Gibson, and T. A. Rijken for helpful discussions. This work was supported by Grants-in-Aid for

Scientific Research from Monbukagakusho of Japan (Nos. 20028007, 21540288, and 21540284). The numerical calculations were performed on the HITACHI SR11000 at KEK.

- 
- [1] T. Motoba, H. Bando, and K. Ikeda, *Prog. Theor. Phys.* **70**, 189 (1980); T. Motoba, H. Bando, K. Ikeda, and T. Yamada, *Prog. Theor. Phys. Suppl.* **81**, 42 (1985).
  - [2] E. Hiyama, M. Kamimura, T. Motoba, T. Yamada, and Y. Yamamoto, *Phys. Rev. C* **53**, 2075 (1996).
  - [3] H. Tamura *et al.*, *Phys. Rev. Lett.* **84**, 5963 (2000).
  - [4] E. Hiyama, Y. Yamamoto, T. A. Rijken, and T. Motoba, *Phys. Rev. C* **74**, 054312 (2006).
  - [5] A. Gal, *Adv. Nucl. Phys.* **8**, 1 (1975).
  - [6] B. F. Gibson and E. V. Hungerford III, *Phys. Rep.* **257**, 349 (1995).
  - [7] A. Nogga, H. Kamada, and W. Glöckle, *Phys. Rev. Lett.* **88**, 172501 (2002).
  - [8] A. R. Bodmer and Q. N. Usmani, *Phys. Rev. C* **31**, 1400 (1985).
  - [9] H. Kanada, T. Kaneko, S. Nagata, and M. Nomoto, *Prog. Theor. Phys.* **61**, 1327 (1979).
  - [10] S. Saito, *Prog. Theor. Phys.* **41**, 705 (1969).
  - [11] B. S. Pudliner, V. R. Pandharipande, J. Carlson, S. C. Pieper, and R. B. Wiringa, *Phys. Rev. C* **56**, 1720 (1997).
  - [12] R. B. Wiringa, V. G. J. Stoks, and R. Schiavilla, *Phys. Rev. C* **51**, 38 (1995).
  - [13] M. M. Nagels, T. A. Rijken, and J. J. deSwart, *Phys. Rev. D* **15**, 2547 (1977); **20**, 1633 (1979).
  - [14] E. Hiyama, M. Kamimura, T. Motoba, T. Yamada, and Y. Yamamoto, *Prog. Theor. Phys.* **97**, 881 (1997).
  - [15] T. A. Rijken, V. G. J. Stoks, and Y. Yamamoto, *Phys. Rev. C* **59**, 21 (1999).
  - [16] E. Hiyama, M. Kamimura, T. Motoba, T. Yamada, and Y. Yamamoto, *Phys. Rev. Lett.* **85**, 270 (2000).
  - [17] J. Simons, *J. Chem. Phys.* **75**, 2465 (1981).
  - [18] D. J. Millener, *Nucl. Phys.* **A804**, 84 (2008).
  - [19] E. Hiyama, M. Kamimura, T. Motoba, T. Yamada, and Y. Yamamoto, *Phys. Rev. C* **66**, 024007 (2002).